

dominates, and that, by the mechanism which is responsible for the Pomernanchuk contribution to the photon cross section,<sup>9,66</sup>

$$\begin{aligned} \frac{1}{\pi}(\sin\pi\alpha)\lambda_{10} &\xrightarrow{\alpha\rightarrow 1} \frac{1}{2}w_1 \neq 0, \\ \frac{1}{\pi}(\sin\pi\alpha)\lambda_1 &\xrightarrow{\alpha\rightarrow 1} 2w_2 \neq 0, \end{aligned} \quad (5.38)$$

<sup>66</sup> H. D. I. Abarbanel *et al.*, Phys. Rev. **160**, 1329 (1967).

we obtain

$$F_1(\rho) \rightarrow w_1\rho, \quad F_2(\rho) \rightarrow w_2. \quad (5.39)$$

There are by now a number of "derivations" of this result,<sup>21,25,62-64</sup> which seems to be in agreement with experiment.

#### ACKNOWLEDGMENTS

The author thanks Alex Dragt and Ching-Hung Woo for useful conversations.

## Meson Regge Exchanges from Simultaneous Analysis of $\pi N$ Scattering Data and Dispersion Sum Rules\*

V. BARGER

*Department of Physics, University of Wisconsin, Madison, Wisconsin 53706*

AND

R. J. N. PHILLIPS

*Rutherford High Energy Laboratory, Chilton, Didcot, Berkshire, England*

(Received 9 June 1969)

An analysis of high-energy  $\pi N$  scattering is made, through the range  $0 \leq -t \leq 2$  ( $\text{GeV}/c$ )<sup>2</sup>, in terms of  $P$ ,  $P'$ ,  $P''$ ,  $\rho$ , and  $\rho'$  Regge poles. High-energy data are supplemented by continuous-moment sum rules that exploit low-energy data through analyticity. Predictions are made for a range of current and future experiments.

### I. INTRODUCTION

THE hypothesis that high-energy scattering may be described by crossed-channel Regge poles has played a valuable role in data analyses, notwithstanding the fact that some branch-cut contributions may be effectively subsumed in the poles. In this paper, we present an analysis of high-energy  $\pi N$  scattering, for  $0 \leq -t \leq 2$  ( $\text{GeV}/c$ )<sup>2</sup>, in terms of the  $P$ ,  $P'$ , ( $P''$ ),  $\rho$ , and  $\rho'$  Regge poles.

Up to about 2 GeV, the  $\pi N$  amplitudes are already known from phase-shift analyses.<sup>1</sup> Through analyticity, this knowledge allows us to put constraints on the high-energy amplitudes, in the form of continuous-moment sum rules (CMSR).<sup>2-4</sup> These CMSR are powerful

tools: They even appear to give a prediction of high-energy scattering on the basis of low-energy data alone. However, we find that such predictions have limited reliability in practice. Since a lot of high-energy data exist, it is better not to ignore them, but rather to include everything in a simultaneous analysis.

In the present work, we use CMSR to supplement high-energy data, for determinations of Regge exchange amplitudes. In particular, the CMSR are crucial in establishing the nature of the  $B^+$  amplitude, and of the  $\rho'$  and  $P''$  contributions.

Beside correlating the existing data in a compact form, our Regge-pole parametrizations lead to interesting predictions of measurements now in progress, notably the high-energy spin-rotation parameters, and the polarization at intermediate energies (2-5 GeV), where duality<sup>3,5</sup> requires that Regge poles give the mean behavior. The model is also extrapolated to

\* Work supported in part by the University of Wisconsin Research Committee with funds granted by the Wisconsin Alumni Research Foundation, and in part by the U. S. Atomic Energy Commission under Contract No. AT(11-1)-881, C00-881-223.

<sup>1</sup> A. Donnachie, R. G. Kirsopp, and C. Lovelace, Phys. Letters **26B**, 161 (1968); A. T. Davies and R. G. Moorhouse, Glasgow University Report (unpublished); A. Donnachie, in *Proceedings of the Fourteenth International Conference on High-Energy Physics, Vienna, 1968*, edited by J. Prentki and J. Steinberger (CERN, Geneva, 1968), p. 139.

<sup>2</sup> K. Igi and S. Matsuda, Phys. Rev. Letters **18**, 625 (1967); A. Logunov, L. Soloviev, and A. Tavkhelidze, Phys. Letters **24B**, 181 (1967).

<sup>3</sup> R. Dolen, D. Horn, and C. Schmid, Phys. Rev. **166**, 1768 (1968).

<sup>4</sup> Y. C. Lin and S. Okubo, Phys. Rev. Letters **19**, 190 (1967); M. G. Olsson, Phys. Letters **26B**, 310 (1967); Phys. Rev. **171**, 1681 (1968); V. Barger and R. J. N. Phillips, Phys. Letters **26B**, 730 (1968); C. Fontan, R. Odorico, and L. Masperi, Nuovo Cimento **58A**, 534 (1968).

<sup>5</sup> G. F. Chew and A. Pignotti, Phys. Rev. Letters **20**, 1078 (1968).

higher energies, to make predictions for 70- and 300-GeV accelerators.

## II. $\pi N$ AMPLITUDES

We use the invariant amplitudes  $A'$  and  $B$ , corresponding to helicity nonflip and flip in the  $t$  channel. It is convenient to take the isospin even and odd combinations

$$A'^{\pm}(\nu, t) = \frac{1}{2} [A'(\pi^- p) \pm A'(\pi^+ p)], \quad (1)$$

with similar definitions for  $B^{\pm}$ . We use the crossing variable  $\nu = (s-u)/(4M)$ . The normal threshold is  $\nu_0 = \mu + t/(4M)$ ;  $s$ ,  $t$ , and  $u$  are the usual invariant squares of energy and momentum transfers;  $M$  and  $\mu$  are the nucleon and pion masses.

We shall consistently use units such that  $\hbar = c = 1$  GeV = 1, except when referring to cross sections, in which case units will be explicitly given.

Regge-pole contributions are parametrized in a form that exhibits their crossing symmetry and also is convenient for CMSR applications:

$$A'^+ = \sum_{i=P, P', P''} [-\gamma_i (\nu_0^2 - \nu^2)^{\alpha_i/2}], \quad (2)$$

$$A'^- = \sum_{i=\rho, \rho'} [-\gamma_i \nu (\nu_0^2 - \nu^2)^{(\alpha_i-1)/2}], \quad (3)$$

$$B^+ = \sum_{i=P, P', P''} \beta_i \nu (\nu_0^2 - \nu^2)^{(\alpha_i-2)/2}, \quad (4)$$

$$B^- = \sum_{i=\rho, \rho'} [-\beta_i (\nu_0^2 - \nu^2)^{(\alpha_i-1)/2}]. \quad (5)$$

Here  $\alpha_i(t)$  denotes the trajectory. The coefficients  $\gamma_i(t)$  and  $\beta_i(t)$  contain the helicity-nonflip and helicity-flip residues, and also the  $1/\sin(\frac{1}{2}\pi\alpha_i)$  or  $1/\cos(\frac{1}{2}\pi\alpha_i)$  factors of the usual Regge parametrization. The characteristic Regge phase factors are included in the powers of  $(\nu_0^2 - \nu^2)$ , that are defined to be real and positive on the real axis between  $\pm\nu_0$ .

The formulas for cross sections and polarization, in terms of  $A'$  and  $B$ , are well known and may be found for example in Ref. 6. This reference also contains an appendix on polarization tensors, and definitions of the various spin rotation parameters.

## III. CONTINUOUS-MOMENT SUM RULES

If a function  $a(\nu)$  is analytic in the cut  $\nu$  plane, is odd under crossing  $\nu \rightarrow -\nu$ , and has a Regge asymptotic expansion for  $\nu \geq \nu_1$

$$a(\nu) = \sum_i [-\lambda_i \nu (\nu_0^2 - \nu^2)^{\theta_i}], \quad (6)$$

then it satisfies the finite-energy sum rule<sup>2</sup>

$$\int_{\nu_0}^{\nu_1} d\nu \operatorname{Im} a(\nu) = \sum_i \frac{1}{2} \lambda_i (\nu_1^2 - \nu_0^2)^{\theta_i+1} \sin(\pi\theta_i) / (\theta_i+1). \quad (7)$$

<sup>6</sup> W. Rarita, R. J. Riddell, Jr., C. B. Chiu, and R. J. N. Phillips, Phys. Rev. **165**, 1615 (1968).

If we multiply  $a(\nu)$  by continuous powers of  $(\nu_0^2 - \nu^2)$ , we can generate a continuous family of moment sum rules.<sup>4</sup>

In the present work, we exploit CMSR for the crossing-odd amplitudes  $\nu A'^+$ ,  $A'^-$ ,  $B^+$ , and  $\nu B^-$ . Typically the  $\nu A'^+$  sum rules take the form

$$\int_{\nu_0}^{\nu_1} d\nu \nu \operatorname{Im} [(\nu_0^2 - \nu^2)^{(-\epsilon-1)/2} A'^+] = \sum_{i=P, P', P''} \gamma_i \frac{(\nu_1^2 - \nu_0^2)^{(\alpha_i - \epsilon + 1)/2} \sin[\frac{1}{2}\pi(\alpha_i - \epsilon - 1)]}{\alpha_i - \epsilon + 1}, \quad (8)$$

where  $\epsilon$  is a continuous parameter. The nucleon-pole contribution is to be included on the left-hand side of Eq. (8).

We evaluate the left-hand side of these CMSR from phase-shift analyses, for a range of  $\epsilon$  values. The upper limit of convergence is  $\epsilon = 1$ . For values of  $\epsilon$  near 1, the lower end of the integration is heavily weighted, and the Regge terms play a relatively small part in satisfying the CMSR. This is undesirable, especially for  $t < 0$ , for which the lower end of the integration is unphysical and the amplitude must be found by extrapolating the phase-shift analysis. The unphysical range is  $\nu_0 \leq \nu \leq [(4\mu^2 - t)(4M^2 - t)]^{1/2}/(4M)$ . When  $t < -4M\mu = -0.52$ , the  $s$ - and  $u$ -channel cuts overlap, so the low-energy part of the integral becomes even more dubious. We suppress this part by taking  $\epsilon \leq -1$ . Large values of  $\epsilon$  are also undesirable, since the amplitude may in practice still contain some non-Regge fluctuations near  $\nu = \nu_1$ ; these will tend to average out in low-moment sum rules, but will distort the higher moments. We therefore restrict  $\epsilon$  to the ranges

$$\begin{aligned} 0 \geq \epsilon \geq -5 & \quad \text{for } t = 0, \\ -1 \geq \epsilon \geq -5 & \quad \text{for } t < 0, \end{aligned} \quad (9)$$

in steps of 0.5 in the first instance. Later, for  $A'^-$  and  $\nu B^-$  sum rules, we further restrict  $\epsilon \geq -3$  (see Sec. IV). We make all evaluations at the same set of  $t$  values:

$$\begin{aligned} 0 \geq t \geq -0.5 & \quad \text{in steps of 0.10,} \\ -0.5 \geq t \geq -0.95 & \quad \text{in steps of 0.15.} \end{aligned} \quad (10)$$

We restrict the use of CMSR to  $-t < 1$ , so that the unphysical range in the integral is not unduly large.

We use the phase-shift results of the CERN and Glasgow groups,<sup>1</sup> going up to laboratory kinetic energies 1.935 and 1.446 GeV, respectively. The corresponding CMSR evaluations prove to be quite compatible, within realistic errors. In final data fitting, therefore, we use exclusively the latest CERN results.<sup>7</sup>

Some general points are worth emphasizing:

(i) The rates of convergence of the Regge series on the right-hand sides of Eqs. (6) and (8) are comparable.

<sup>7</sup> C. Lovelace (private communication).

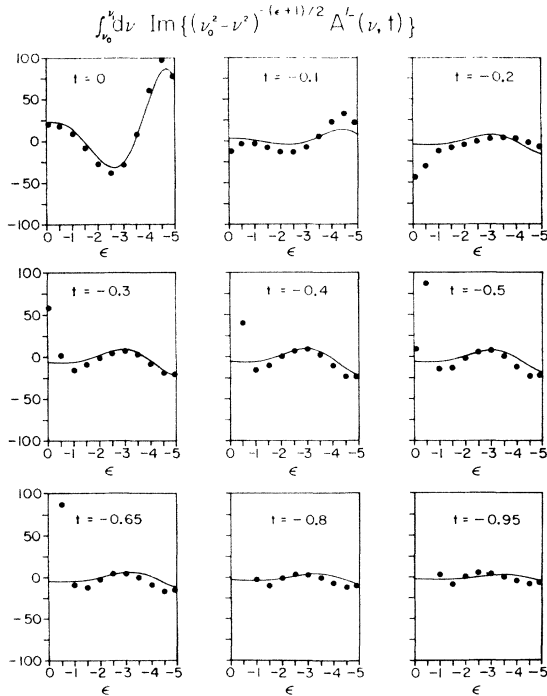


FIG. 1. Continuous-moment sum rules (CMSR) for the  $A'^-$  amplitude. The solid dots represent the CMSR low-energy integrals from CERN phase shifts (Ref. 7). The solid curves illustrate results of our  $\rho, \rho'$  Regge fit to CMSR and high-energy scattering data.

A particular Regge pole is about as important in the CMSR, taken together, as it is in fitting the Regge amplitude at  $\nu = \nu_1$ .

(ii) Since we are obliged to take  $\nu_1$  rather small ( $\nu_1 = 2.1$  or  $1.5$  GeV for the phase shifts used), lower-lying Regge singularities will play a bigger role in the CMSR than they do in scattering data in the normally accepted exclusively Regge region  $\nu > 5$  GeV.

(iii) For Regge analyses, sum rules effectively extended the energy range down to  $\nu_1$ , providing a larger lever arm in  $\nu$ .

(iv) Because sum rules tend to average over non-Regge fluctuations, it is safer to use CMSR at  $\nu_1 = 2$  GeV than to use scattering data at these energies, in a Regge-pole analysis.

(v) A big advantage of sum rules is that they relate directly to amplitudes, rather than to quadratic functions of amplitudes, as with scattering data. They exploit the unscrambling of quadratics that has already been done in the low-energy phase-shift analyses.

(vi) By inverting Eq. (8), given the left-hand side, one can apparently predict high-energy scattering from low-energy amplitudes. In principle, one can indeed continue an analytic function from one region to another, and the CMSR give one prescription for doing

this. In practice, however, there are errors coming from the low-energy amplitudes themselves, from the truncation of the Regge series, etc. Any predictions can only be approximate; we may test their accuracy by comparing them with actual high-energy data.

#### IV. METHOD OF ANALYSIS

We analyze CMSR and high-energy scattering data together, using three complementary approaches:

(i) Analysis at fixed  $t$  values [at the points defined in Eq. (10)]. No assumptions about the  $t$  dependence of Regge parameters are then needed. Scattering data are interpolated where necessary.

(ii) Analysis over a range of  $t$ , parametrizing the  $\alpha_i, \beta_i, \gamma_i$  by polynomials in  $t$ . This imposes continuity, with the minimum of assumptions about  $t$  dependence, but the polynomials tend to blow up outside the range considered.

(iii) Analysis over a range of  $t$ , parametrizing with smooth functions such as  $e^{at}$  or  $(t-t_0)e^{at}$ . The advantage here is a smoother extrapolation in  $t$ . The difficulty lies in knowing what functions to use; previous experience with approaches (i) or (ii) is essential.

We made many fits to data with all three approaches. The most satisfactory of these are described later.

The isospin-1 exchanges are first analyzed separately. We use the  $A'^-$  and  $B^-$  CMSR, plus the following

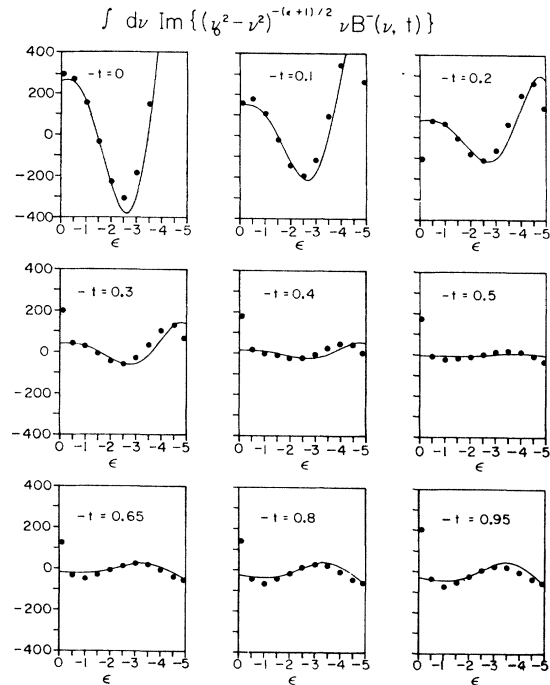


FIG. 2. CMSR and  $\rho, \rho'$  Regge fit for  $B^-$  amplitude (cf. Fig. 1 caption).

scattering data:

$$\Delta\sigma_t = \sigma_t(\pi^-p) - \sigma_t(\pi^+p),$$

8–22 GeV/c, from Ref. 8

$$d\sigma/dt(\pi^-p \rightarrow \pi^0n), \quad 5\text{--}18 \text{ GeV/c},$$

$0 \leq -t \leq 2(\text{GeV/c})^2$ , from Ref. 9

$P(\pi^-p \rightarrow \pi^0n)$  at 5.1, 5.9, and 11.2 GeV/c,

$0 \leq -t \leq 2$ , from Ref. 10.

The difference  $[d\sigma/dt(\pi^-p) - d\sigma/dt(\pi^+p)]$  contains further information about  $I=1$  exchanges, but this is an interference effect and depends also on  $I=0$  exchanges. We content ourselves with checking subsequently that this is correctly given.

Having decided upon a solution for the  $I=1$  exchange parameters, we fix them and analyze the remaining data to find  $I=0$  exchanges. These data are the  $A^{+4}$  and  $B^+$  CMSR, together with

$\sigma_t(\pi^\pm p)$ , 7–23 GeV/c, from Ref. 8

$\alpha(\pi^\pm p)$ , 7–28 GeV/c, from Ref. 8

$d\sigma/dt(\pi^\pm p)$ , 5–26 GeV/c, from Refs. 11 and 12

$P(\pi^\pm p)$ , 5–12 GeV/c, from Refs. 13 and 14.

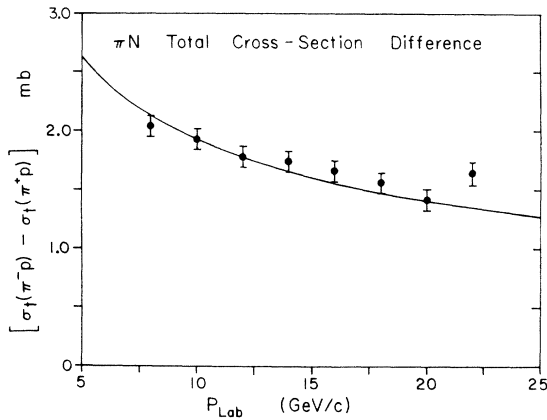


FIG. 3.  $\rho, \rho'$  Regge fit to  $\Delta\sigma_t = [\sigma_t(\pi^-p) - \sigma_t(\pi^+p)]$ . Data from Ref. 8.

<sup>8</sup> K. J. Foley *et al.*, Phys. Rev. Letters **19**, 330 (1967); **19**, 193 (1967).

<sup>9</sup> O. Guisan (private communication); the high-energy charge-exchange data from this source are an amended version of previously published Saclay-Orsay results [A. V. Stirling *et al.*, Phys. Rev. Letters **14**, 763 (1965); P. Sonderegger *et al.*, Phys. Letters **20**, 75 (1966)]; M. A. Wahlig and I. Mannelli, Phys. Rev. **168**, 1515 (1968); A. S. Carroll, I. F. Corbett, C. J. S. Damerell, N. Middlemas, D. Newton, A. B. Clegg, and W. S. C. Williams, *ibid.* **177**, 2047 (1969).

<sup>10</sup> P. Bonamy *et al.*, in *Proceedings of the Heidelberg International Conference on Elementary Particles, Heidelberg, Germany, 1967*, edited by H. Filthuth (North-Holland Publishing Company, Amsterdam, 1968), p. 171; D. Drobnis *et al.*, Phys. Rev. Letters **20**, 274 (1968).

<sup>11</sup> K. J. Foley *et al.*, Phys. Rev. Letters **11**, 425 (1963); Phys. Rev. **181**, 1775 (1969). Data from this reference were restricted to  $|t| > 0.05$  in the fits to avoid Coulomb interference effects.

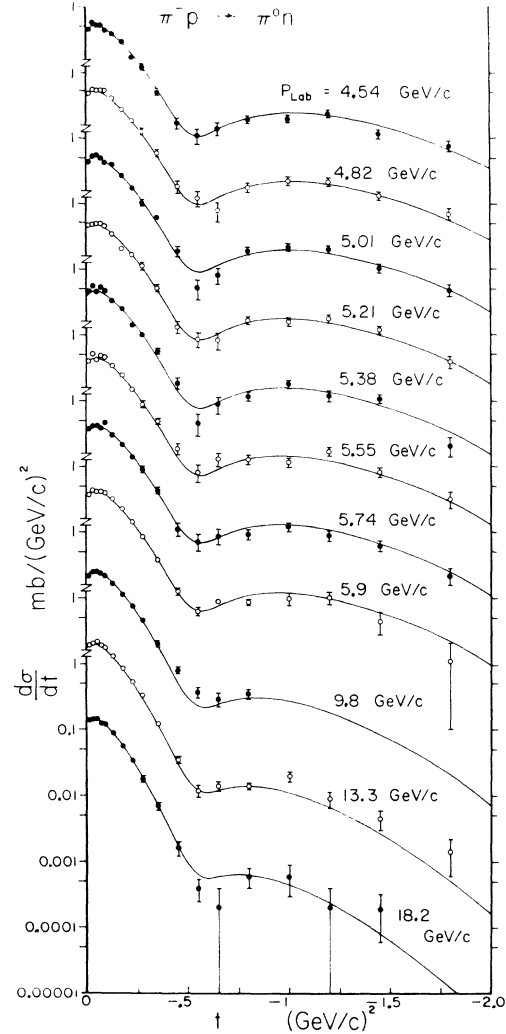


FIG. 4. Results of  $\rho, \rho'$  Regge-pole fit to  $d\sigma/dt(\pi^-p \rightarrow \pi^0n)$  data above 5 GeV/c. Data from Guisan *et al.*, Ref. 9.

## V. RESULTS

### A. Isospin-1 Exchanges

A preliminary account of this part has already been published.<sup>15</sup> Our present results differ in that the  $t$  range is extended, the latest CERN phase shifts are incorporated, and the charge-exchange polarization data are included in the fitting (formerly they were predicted). We find the following general properties:

(i) The  $\rho$  and  $\rho'$  parameters tend to be correlated. However, if we assume that the trajectories are spaced

<sup>12</sup> D. P. Owen *et al.*, Phys. Rev. **181**, 1794 (1969); J. Orear *et al.*, Nuovo Cimento **38**, 60 (1965); C. T. Coffin *et al.*, Phys. Rev. **159**, 1169 (1963); D. Harting *et al.*, Nuovo Cimento **38**, 60 (1965).

<sup>13</sup> M. Borghini *et al.*, Phys. Letters **24B**, 77 (1967).

<sup>14</sup> R. J. Esterling *et al.*, Phys. Rev. Letters **21**, 1410 (1969).

<sup>15</sup> V. Barger and R. J. N. Phillips, Phys. Rev. Letters **21**, 865 (1968).

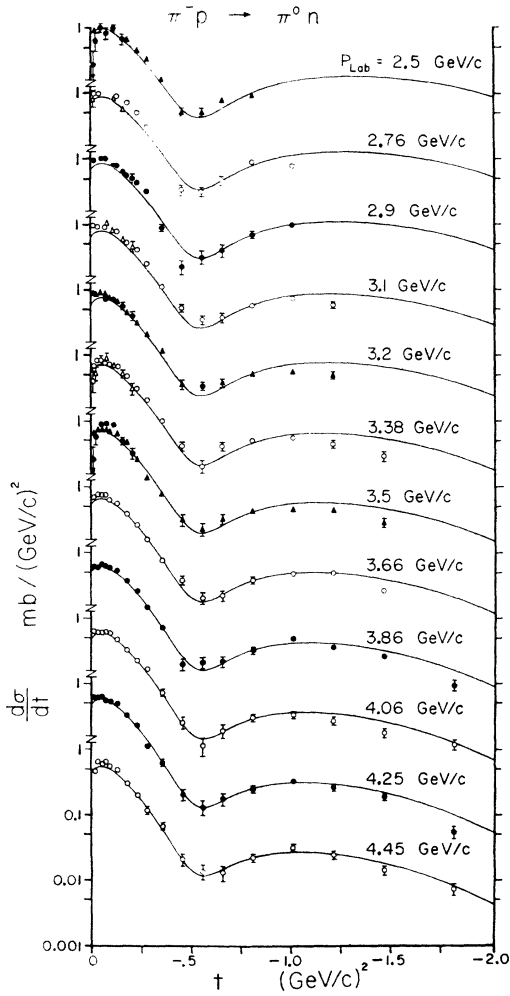


FIG. 5. Extrapolations of  $\rho, \rho'$  Regge model to the intermediate laboratory momentum range. Data from Ref. 9.

well apart and have similar slopes, it becomes possible to separate the  $\rho$  and  $\rho'$  contributions to the amplitudes. This we do.

(ii)  $\beta_\rho$  has the conventional nonsense wrong-signature zero at  $\alpha_\rho=0$ .

(iii)  $\gamma_\rho$  has the usual "crossover zero"<sup>16</sup> near  $t=-0.15$ , but no zero at  $\alpha_\rho=0$ . We constructed some solutions in which the crossover zero was displaced to  $\alpha=0$ , or in which an extra zero was simply imposed, but the quality of the fits to data was inferior.

(iv) For  $\rho'$  the parameters  $\alpha, \beta$ , and  $\gamma$  all tend to vanish near  $t=0$ . For simplicity, therefore, we parametrize them to vanish exactly there. Many variants of this solution can be constructed, by displacing one or more of these zeros, and the fit to data can even be improved slightly in this way. But all these modified solutions remain close to the original. Possible reasons

<sup>16</sup> V. Barger and L. Durand, III, Phys. Rev. Letters **19**, 1295 (1967); R. J. N. Phillips and W. Rarita, Phys. Rev. **139**, B1336 (1965).

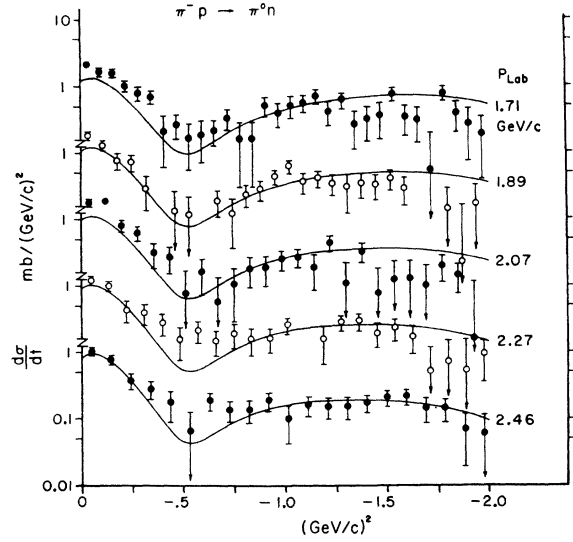


FIG. 6. Comparison of  $\rho, \rho'$  Regge-model extrapolations with fairly low-energy  $\pi^-p \rightarrow \pi^0n$  scattering data from Carroll *et al.*, Ref. 9.

for this behavior include (a)  $\rho'$  choosing nonsense at  $\alpha_{\rho'}=0$  and (b)  $\rho'$  conspiring at  $t=0$ .

Our best fit of this kind is the following:

$$\begin{aligned} \alpha_\rho(t) &= 0.55 + t, \\ \alpha_{\rho'}(t) &= t, \\ \beta_\rho(t) &= -(24.6 + 58.7e^{1.29t})\Gamma(1 - \alpha_\rho) \sin(\frac{1}{2}\pi\alpha_\rho), \\ \beta_{\rho'}(t) &= -293.8te^{5.0t}, \\ \gamma_\rho(t) &= 3.94(1 + 6.0t)e^{2.55t}\Gamma(-\alpha_\rho) \sin(\frac{1}{2}\pi\alpha_\rho), \\ \gamma_{\rho'}(t) &= -74.8t(1 + 2.45t)e^{4.78t}. \end{aligned}$$

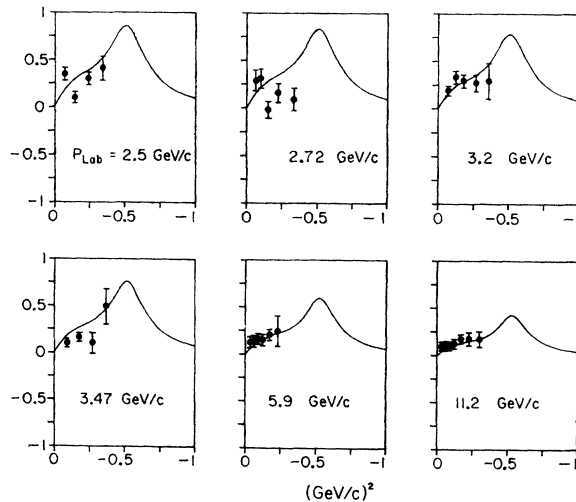


FIG. 7.  $\rho, \rho'$  Regge-model description of  $\pi^-p \rightarrow \pi^0n$  polarization data from Ref. 10. Only data above 5 GeV/c were included in the fit.

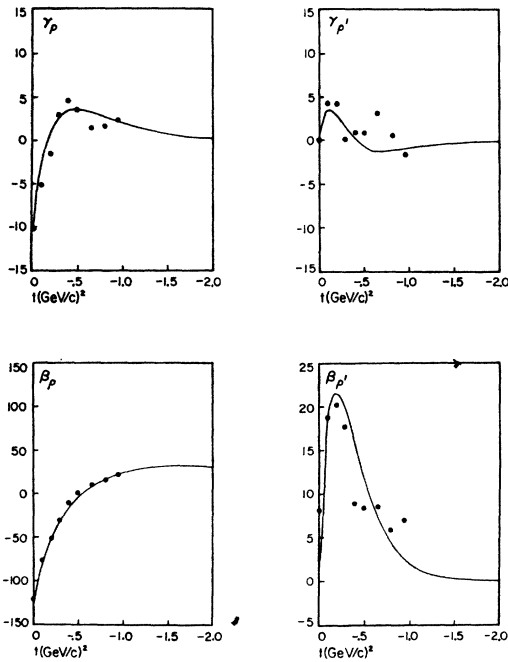


FIG. 8.  $\rho, \rho'$  Regge residues obtained from analysis at fixed  $t$  values are denoted by the solid points. The curves represent the results of the final fitted solution [cf. Eqs. (3) and (5) for residue definitions].

(Three-figure accuracy is given simply to allow our solution to be reconstructed.) The sine and  $\Gamma$  factors in the  $\rho$  coefficients correspond exactly, in our notation, to the conventional treatment of nonsense wrong-signature zeros by a  $\Gamma$  function in the residue.<sup>17</sup> In the case of  $\rho'$ , where identification with a real Regge pole is more questionable, we have used a simpler form. The behavior near  $\alpha_{\rho'} = -1$  is ill determined; in the solution above, the  $\rho'$  contributions are in any case small near this point, and beyond.

This solution gives  $\chi^2=278$  for a set of 254 data (CMSR and high-energy scattering) in the range  $0 \leq -t \leq 1$ , and a further  $\chi^2=22$  for 23 data in the range  $1 < -t < 2$ .

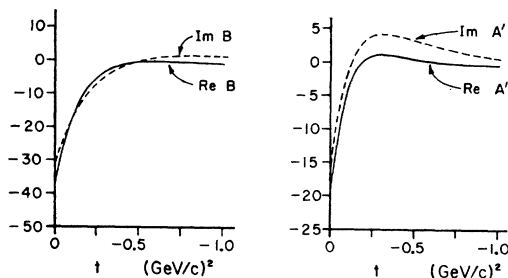


FIG. 9. Reconstructed  $A'$  and  $B$  amplitudes for  $\pi^- p \rightarrow \pi^0 n$  at 6 GeV/c from  $\rho, \rho'$  Regge fit.

<sup>17</sup> J. E. Lang, University of Illinois Report, 1968 (unpublished).

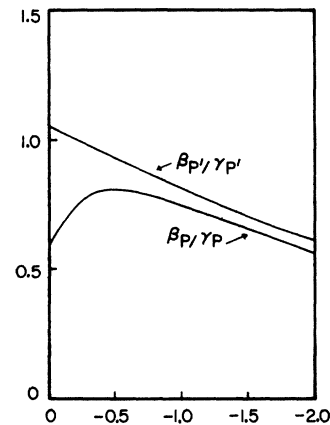


FIG. 10.  $\beta_i/\gamma_i$  residue ratios from a fit with  $P, P' I=0$  Regge-pole exchanges [cf. Eqs. (2) and (4) for residue definitions].

The CMSR data for the  $I=1$  exchange amplitudes are shown in Figs. 1 and 2, along with the  $\rho+\rho'$  fits which are represented by the solid curves. The comparisons of the fits with the data on  $\Delta\sigma, d\sigma/dt(\pi^- p \rightarrow \pi^0 n)$  and  $P(\pi^- p \rightarrow \pi^0 n)$  are given in Figs. 3-7. The results of this fit to the CMSR and the scattering data above 5 GeV/c extrapolate remarkably well through the scattering data in the 2-5-GeV/c momentum range. The residues obtained from the fixed- $t$  analyses are compared with the final  $\rho+\rho'$  solution in Fig. 8. The resultant  $A'^-$  and  $B^-$  amplitudes at 6 GeV/c from  $\rho+\rho'$  exchange are illustrated in Fig. 9.

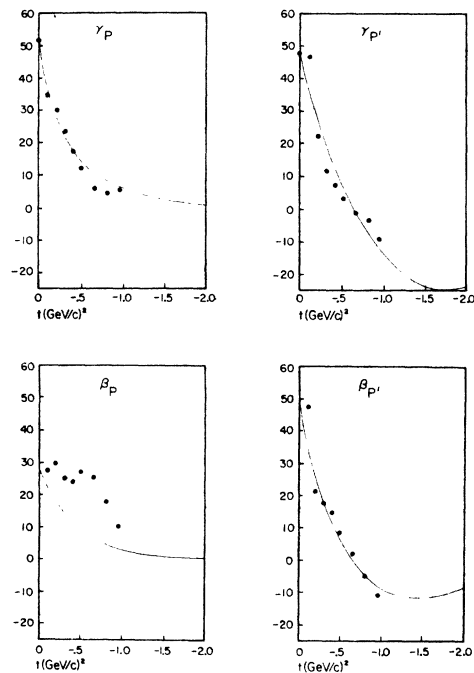


FIG. 11.  $P, P'$  Regge residues from fixed- $t$  analysis (solid points) are compared with results of parametrized fit (curves).

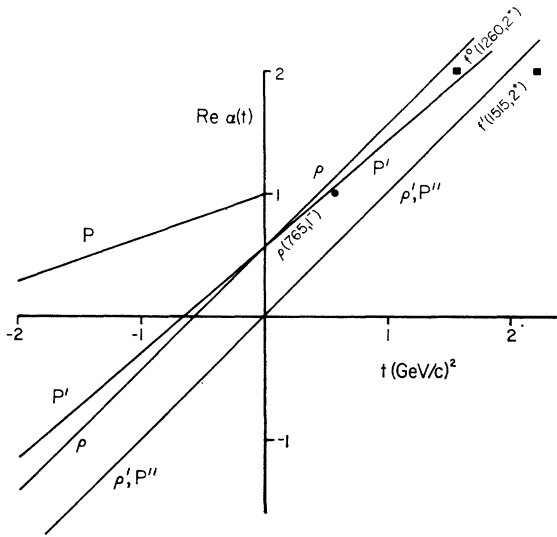


FIG. 12. Spin-mass plot of straight-line Regge trajectories deduced from our fit to  $\pi N$  data for  $t \leq 0$ .

In contrast to the above sense-choosing  $\rho$  solution, the solutions we constructed in which  $\rho$  chooses nonsense at  $\alpha=0$  all had  $\chi^2 > 400$ , for the full data set. This hypothesis is clearly less successful, at least with the parametrizations we tried.

Derem<sup>18</sup> has recently presented a Regge  $\rho + \rho'$

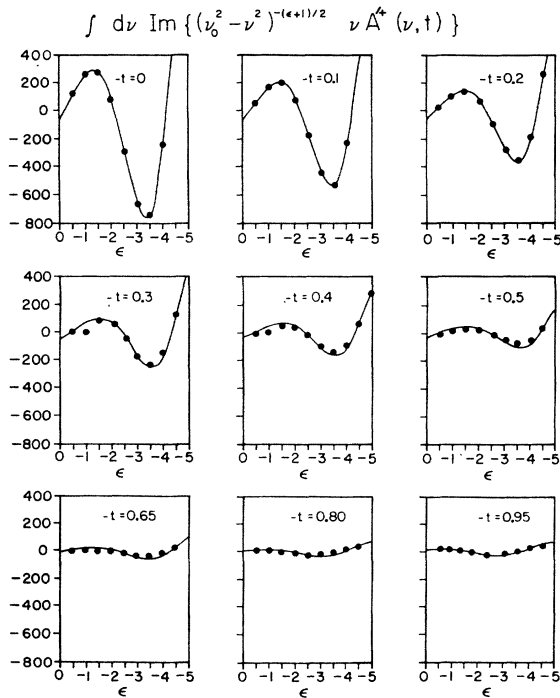


FIG. 13. CMSR and  $P, P', P''$  Regge fit for  $A^{++}$  amplitude (cf. Fig. 1 caption).

<sup>18</sup>A. Derem, Saclay Report, 1969 (unpublished).

analysis of charge-exchange data, for  $0 \leq -t \leq 1$ , without any CMSR. He found acceptable fits with five different models and concluded *inter alia* that one cannot decide whether  $\rho$  chooses nonsense at  $\alpha=0$  or not. We have tested his models against our more extensive data set, including CMSR, and find the following:

(i) Only Derem's solution 4 is successful for  $-t > 1$ ; however, he used no data in this range.

(ii) Confining ourselves to  $0 \leq -t \leq 1$ , Derem's solutions 1a, 1b, 2, 3, and 4 give  $\chi^2 = 277, 264, 280, 236$ , and 210, respectively, for the scattering data, and  $\chi^2 = 248, 263, 177, 118$ , and 116, respectively, for the CMSR. The corresponding numbers for our solution above are  $\chi^2 = 208$  and 69.

(iii) Our data set thus prefers Derem's solutions 3 and 4; these are both cases in which  $\rho$  does not choose nonsense, and which resemble our solution above. This preference stems largely from the  $B^-$  CMSR. The  $A^{+-}$  CMSR are more directly affected by nonsense choosing, and also give a preference for solutions 3 and 4; however, big errors are assigned here because there are substantial cancellations within the low-energy integrals, so these CMSR carry little weight in  $\chi^2$ .

Finally, two remarks about the CMSR for  $A^{+-}$  and  $B^-$ . We noticed that the higher moments were not entirely consistent with the lower moments. Since there

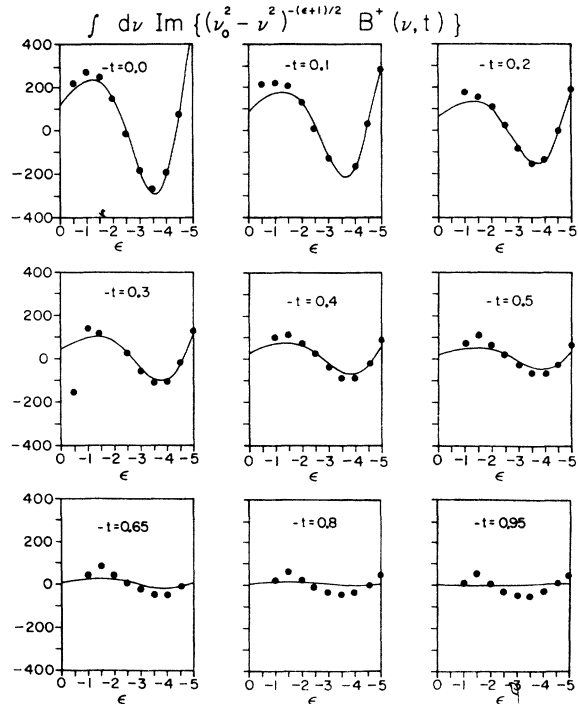


FIG. 14. CMSR and  $P, P', P''$  Regge fit for  $B^+$  amplitude (cf. Fig. 1 caption).

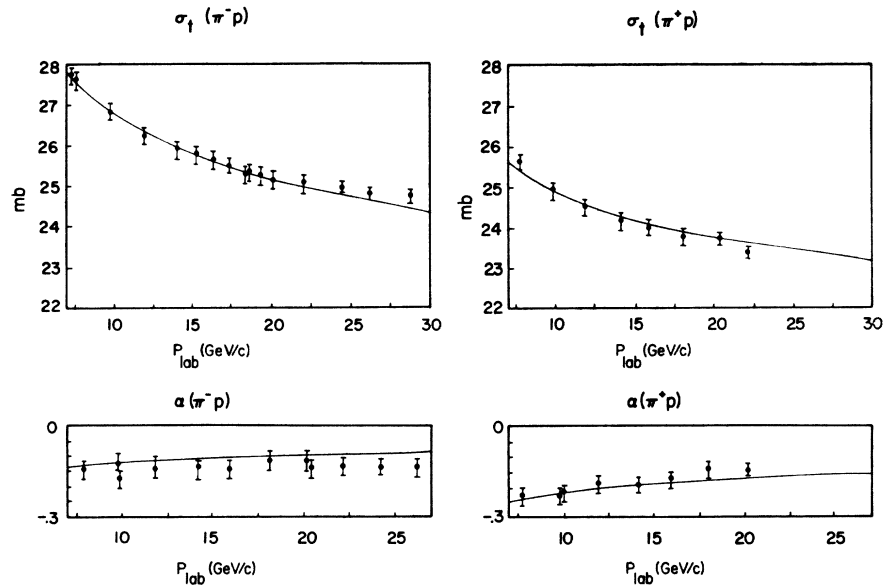


FIG. 15. [ $P, P', P'', \rho, \rho'$ ] Regge-pole fit to  $\sigma_t$  and  $\alpha = (\text{Re}A'/\text{Im}A')_{t=0}$  data from Ref. 8.

appear to be some energy-dependent fluctuations in the data even above 2 GeV, we conclude that the higher-moment CMSR might be unreliable and dropped those with  $|\epsilon| > 3$ .

It is interesting to see how consistently one can predict high-energy scattering from CMSR and low-energy phase shifts alone. To this end, we predicted the total cross-section difference  $\Delta\sigma = [\sigma_t(\pi^-p) - \sigma_t(\pi^+p)]$  at 5, 10, and 20 GeV/c, from a one-pole fit to  $A'^-$  CMSR at  $t=0$ . The results of using CERN I phase shifts<sup>1</sup> with a range of cutoff values  $\nu_1$  are shown in Table I; experimental values are also shown. Such results show that CMSR must be used judiciously, to supplement rather than to replace high-energy data.

### B. Isospin-0 Exchanges

This part of the work falls into two subsections: a fit to data with  $P+P'$  alone, and a fit including a  $P''$  Regge pole.

With  $P+P'$ , we find the following properties, some of which were indicated in an earlier study of CMSR alone<sup>19</sup>:

(i)  $\gamma_{P'}$  has a zero near  $t = -0.6$ . If this coincides with the point  $\alpha_{P'} = 0$ , it corresponds to a double zero in the conventional residue function, such as occurs in the "no-compensation mechanism,"<sup>20</sup> or in the empirical cyclic residue structure suggested by the present authors.<sup>21,22</sup>

<sup>19</sup> V. Barger and R. J. N. Phillips, Phys. Letters **26B**, 730 (1968).

<sup>20</sup> C. B. Chiu, S. Y. Chu, and L. L. Wang, Phys. Rev. **161**, 1563 (1967).

<sup>21</sup> V. Barger and R. J. N. Phillips, Phys. Rev. Letters **20**, 564 (1968).

<sup>22</sup> V. Barger and R. J. N. Phillips, Phys. Rev. Letters **22**, 116 (1969).

(ii) The spin-flip coefficients tend to follow, at least qualitatively, the relation  $B^+ \approx A'^+/\nu$  (and hence  $\beta_i \approx \gamma_i$ ), previously suggested by the CMSR.<sup>19</sup> The  $\beta_i/\gamma_i$  ratios from a representative  $P+P'$  fit are illustrated in Fig. 10.

(iii)  $\beta_{P'}$  has a zero near that of  $\gamma_{P'}$ . This is forced by the approximate mirror symmetry of high-energy  $\pi^+p$  and  $\pi^-p$  polarizations.<sup>14,22</sup>

(iv)  $\alpha_P$  has a small slope, of the order of 0.2-0.4.<sup>23</sup> This may be seen as follows. The forward  $\pi N$  cross section falls with energy,  $d\sigma/dt(0) \sim s^{-0.3}$  at accelerator energies. The  $s$  dependence is similar near  $t = -0.6$  (no shrinking of the forward peak), but here the  $P'$  contributions are negligible; hence  $\alpha_P(-0.6) \approx 0.85$ .

(v) The  $B^+$  CMSR cannot be well fitted by  $P+P'$ . These CMSR are fairly sensitive to details of the low-energy phase shifts, and this could be the explanation. They are also more sensitive to lower-lying Regge terms, than the high-energy data; this suggests an alternative explanation, in terms of  $P''$ .

TABLE I. Predictions of  $\Delta\sigma$  from CMSR alone.

$\nu_1$	$\Delta\sigma(P_{\text{lab}}=5 \text{ GeV}/c)$ (mb)	$\Delta\sigma(10 \text{ GeV}/c)$ (mb)	$\Delta\sigma(20 \text{ GeV}/c)$ (mb)
1.585	1.80	1.48	1.21
1.705	1.62	1.41	1.22
1.765	1.65	1.44	1.26
1.885	1.88	1.62	1.39
2.015	2.22	1.83	1.51
2.075	2.34	1.89	1.52
Experiment	$2.64 \pm 0.02$	$1.93 \pm 0.09$	$1.42 \pm 0.09$

<sup>23</sup> The exact slope that we obtain for  $\alpha_P$  is dependent upon the relative importance assigned to different data sets. The new and old  $\pi p$  data of Foley *et al.* [Ref. 11] are somewhat inconsistent. We have assigned equal weight to all  $d\sigma/dt$  elastic data in the final analysis.



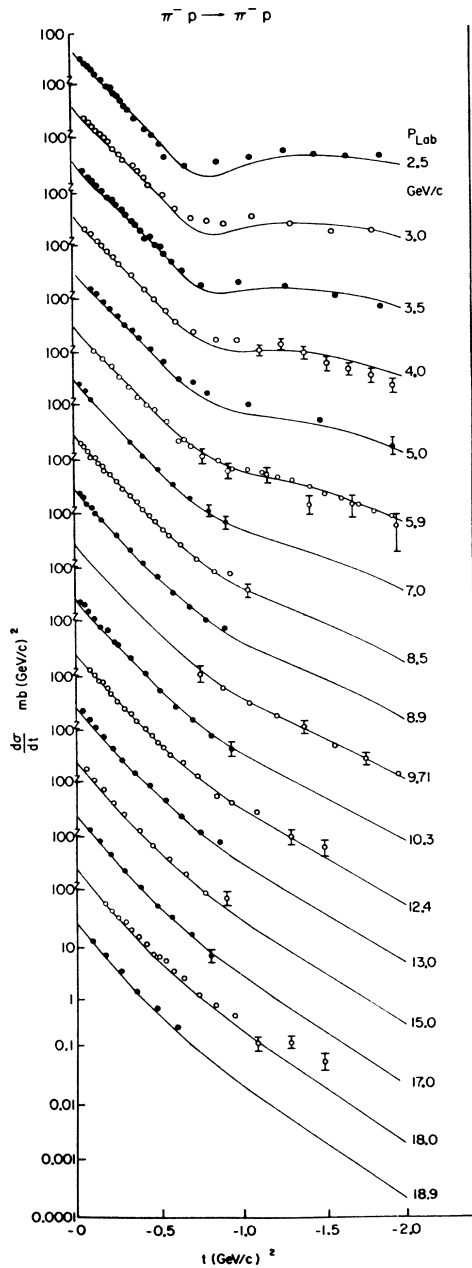


FIG. 16. Fit to  $d\sigma/dt(\pi^-p)$  data above 5 GeV/c with  $[P, P', P'', \rho, \rho']$  Regge model. Extrapolations to lower momenta are also shown. Data from Refs. 11 and 12.

A typical fit to data with  $P+P'$  is the following:

$$\alpha_P = 1 + 0.37t,$$

$$\alpha_{P'} = 0.57 + 0.86t,$$

$$\beta_P = 31.0e^{2.09t},$$

$$\beta_{P'} = 41.1e^{0.39t} \sin\left(\frac{1}{2}\pi\alpha_{P'}\right) [\Gamma(1 - \frac{1}{2}\alpha_{P'})]^2,$$

$$\gamma_P = 20.8e^{6.5t} + 31.7e^{1.82t},$$

$$\gamma_{P'} = (21.7 + 17.1e^{0.32t}) \sin\left(\frac{1}{2}\pi\alpha_{P'}\right) [\Gamma(1 - \frac{1}{2}\alpha_{P'})]^2.$$

In the  $P'$  terms, the sine factor gives recurring zeros, as conjectured in Refs. 21 and 22; the  $\Gamma$  factor reinstates poles at  $\alpha=2, 4, \dots$ , etc. The residues from the fixed- $t$  analysis are compared with this  $P+P'$  solution in Fig. 11.

When  $P''$  is added to the analysis, we find further:

(vi) Introducing  $\beta_{P''}$  gives a big improvement in fitting both the  $B^+$  CMSR and the elastic  $\pi p$  polarization data. A relatively strong  $P''$  contribution is indicated.

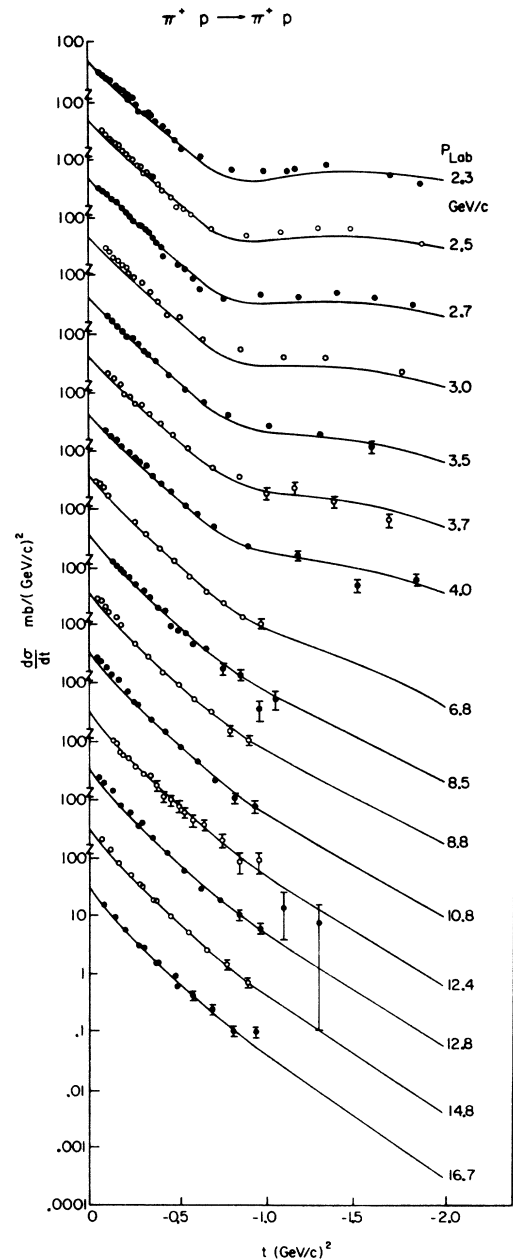


FIG. 17. Fit to  $d\sigma/dt(\pi^+p)$  data (cf. Fig. 16 caption).

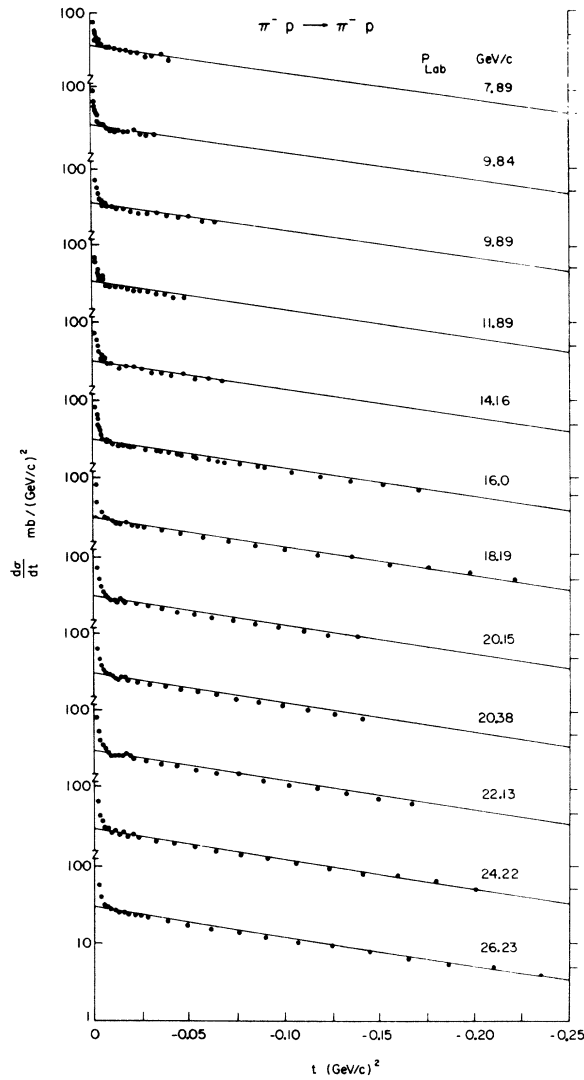


FIG. 18. [ $P, P', P'', \rho, \rho'$ ] Regge-pole fit to recent  $d\sigma/dt(\pi^- p)$  data from Ref. 11.

(vii) Introducing  $\gamma_{P''}$  gives little improvement in the fit to CMSR and data; they give rather a poor determination of  $\gamma_{P''}$ , and it remains consistent with zero.

We therefore decide to ignore  $\gamma_{P''}$ . Our best fit to data with the remaining  $P+P'+P''$  parameters is the following:

$$\begin{aligned} \alpha_P &= 1 + 0.36t, \\ \alpha_{P'} &= 0.56 + 0.86t, \\ \alpha_{P''} &= t, \\ \beta_P &= 42.5e^{2.45t}, \\ \beta_{P'} &= 24.7e^{0.17t} \sin(\frac{1}{2}\pi\alpha_{P'}) [\Gamma(1 - \frac{1}{2}\alpha_{P'})]^2, \\ \beta_{P''} &= 49.8e^{2.31t}, \\ \gamma_P &= 21.6e^{6.5t} + 31.1e^{1.81t}, \\ \gamma_{P'} &= (22.2 + 16.9e^{0.34t}) \sin(\frac{1}{2}\pi\alpha_{P'}) [\Gamma(1 - \frac{1}{2}\alpha_{P'})]^2. \end{aligned}$$

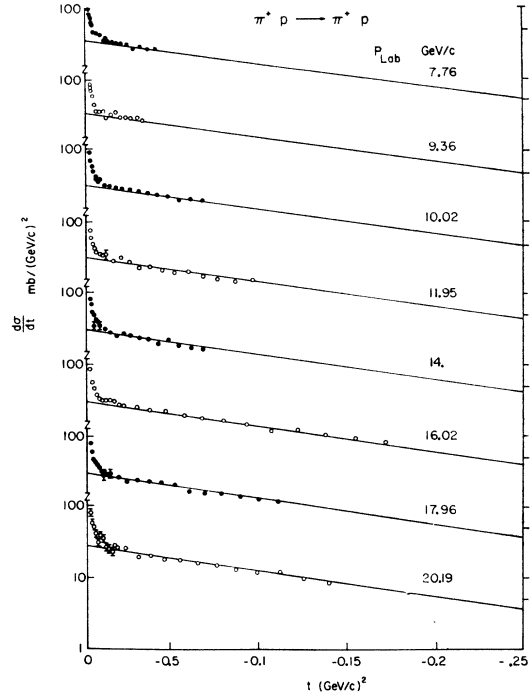


FIG. 19. Fit to recent  $d\sigma/dt(\pi^+ p)$  data (cf. Fig. 18 caption).

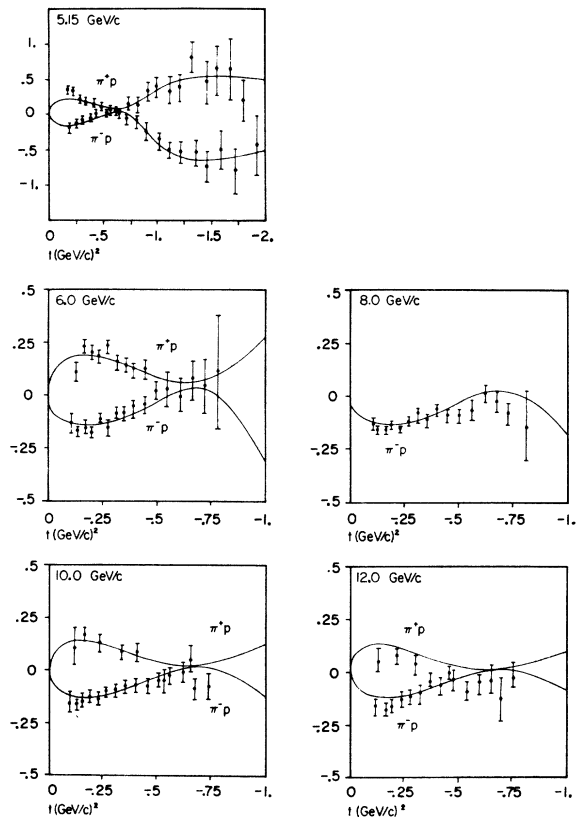


FIG. 20. [ $P, P', P'', \rho, \rho'$ ] Regge-model description of  $\pi^\pm p$  polarization data from Refs. 13 and 14.

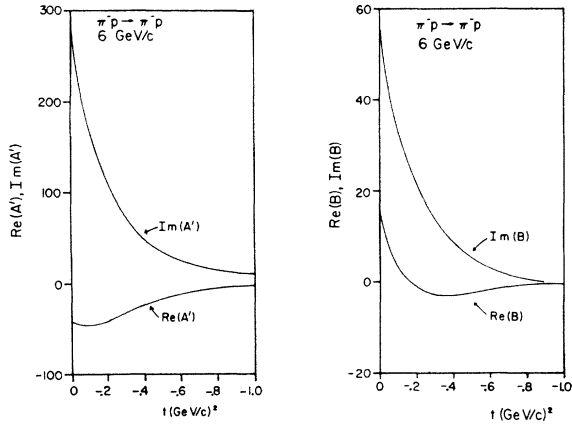


FIG. 21. Reconstruction of  $A'$  and  $B$  amplitudes for  $\pi^-p \rightarrow \pi^-p$  at 6 GeV/c from  $[P, P', P'', \rho, \rho']$  Regge-pole fit.

The  $P''$  trajectory form obtained from this analysis coincides remarkably well with the expected trajectory for the  $f'(1515, 2^+)$  meson, as illustrated in Fig. 12.

The  $P, P', P''$  fit to the CMSR data for  $I=0$  exchange are illustrated in Figs. 13 and 14. The corresponding comparisons with the  $\sigma_t(\pi^\pm p)$ ,  $\alpha(\pi^\pm p)$ ,  $d\sigma/dt(\pi^\pm p)$ , and  $P(\pi^\pm p)$  data are given in Figs. 15–20. The  $A'$  and  $B$  amplitudes for  $\pi^-p$  scattering resulting from the  $P, P', P'', \rho, \rho'$  solution are illustrated in Fig. 21. An interesting conclusion is that the ratio  $\text{Re}A'/\text{Im}A'$  shows an appreciable variation with  $t$ .

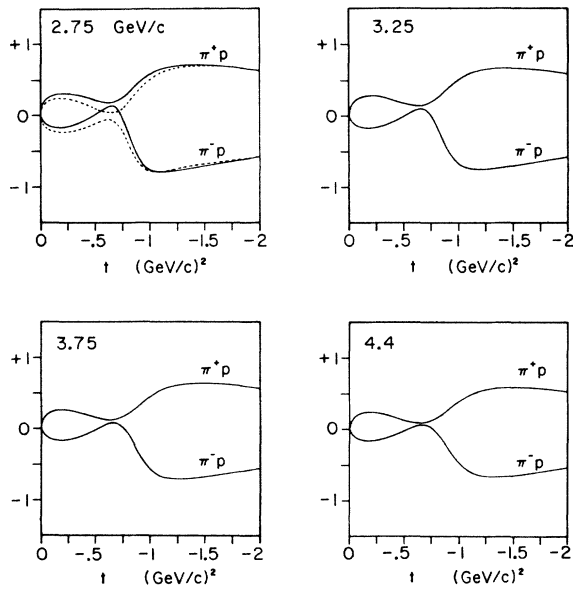


FIG. 22. Predictions for  $\pi^\pm p$  elastic polarization at intermediate laboratory momenta based on the  $[P, P', P'', \rho, \rho']$  Regge-pole fit to CMSR and high-energy scattering data. The dashed curves at the lowest momentum illustrate the corresponding prediction from a (poorer) fit to the data with no  $P''$  amplitude included.

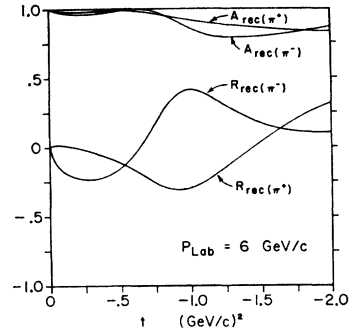


FIG. 23. Predictions for the spin-rotation parameters  $R_{\text{recoil}}$  and  $A_{\text{recoil}}$  at 6 GeV/c for  $\pi^\pm p$  elastic scattering.

## VI. PREDICTIONS

We illustrate some of the more interesting predictions, for our  $P, P', P''$  solution. Using our formulas, the reader can readily compute other cases for himself.

First it is interesting to examine the intermediate range 2–5 GeV/c, where non-Regge fluctuations may appear but where the duality hypothesis<sup>3,5</sup> requires that Regge poles should give the mean behavior. That this is so for cross sections is already shown in Figs. 4–6 and 16–19; our predictions for elastic polarization are given in Fig. 22.

At higher energies, polarization is approximately odd (i.e., mirror symmetric) between  $\pi^+p$  and  $\pi^-p$ , and the two curves touch near  $t=-0.6$ . This is easily explained in terms of the dominant  $P, P'$ , and  $\rho$  terms<sup>22</sup>; the even contributions to  $Pd\sigma/dt$  come from  $P$ - $P'$  interference, and can be arranged to cancel out; the odd contributions come from  $\rho$ - $P$  and  $\rho$ - $P'$  interference, and

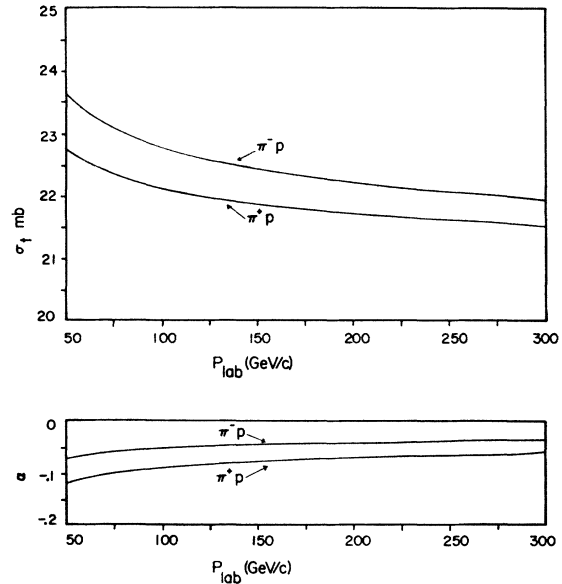


FIG. 24. Extrapolations of our Regge-pole solution to the 50–300-GeV/c range for total cross sections and  $\alpha = (\text{Re}A'/\text{Im}A')_{t=0}$ .

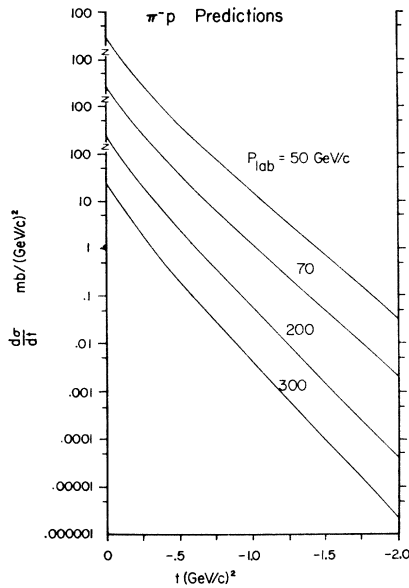


FIG. 25. Predictions of  $d\sigma/dt(\pi^-p)$  for momenta between 50 and 300 GeV/c.

have approximate double zeros near  $t = -0.6$  because of phase and ghost-eliminating factors.<sup>22</sup> At lower energies, however,  $P''$  becomes more important and changes this simple picture. The principal effect is  $B(P'') - A'(P+P')$  interference, which gives an even contribution not vanishing near  $t = -0.6$ . As a result,  $\pi^+p$  and  $\pi^-p$  polarizations obey a kind of distorted mirror symmetry; the curves still touch near  $t = -0.6$ , but the mean value is displaced upward from zero more and more as energy decreases. Polarization data in the 2–5-GeV/c range are meager,<sup>24</sup> but a new  $\pi^\pm p$  experiment at Argonne is currently in the final analysis stage.<sup>25</sup>

Another interesting prediction is that of spin-rotation parameters, because the latter will give a direct measure of the spin dependence of  $P$  and  $P'$  terms. Other data give an incomplete picture. Measurements of  $d\sigma/dt$  show that  $B(P+P')$  is not so strong as to give an anomalous angular distribution at small  $t$ .<sup>26</sup> Measurements of polarization show that  $P-P'$  interference cancels out, so that  $(B/A')_P \approx (B/A')_{P'}$ ; this still

<sup>24</sup> O. Chamberlain *et al.*, Phys. Rev. Letters **17**, 975 (1966).

<sup>25</sup> G. Conforto and A. Yokasawa (private communication).

<sup>26</sup> C. Michael, Phys. Letters **26B**, 392 (1968).

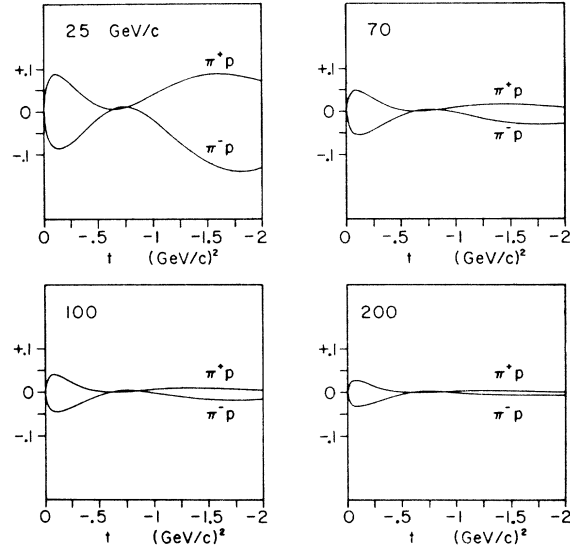


FIG. 26. Predictions of  $\pi^\pm p$  elastic polarization at momenta corresponding to Serpukhov and Batavia accelerators.

leaves great freedom. In our present analysis, the ratios  $B/A$  are determined by CMSR, but they can also be measured directly through rotation parameters.

Figure 23 shows our predictions for the rotation parameters  $R_{\text{recoil}}$  and  $A_{\text{recoil}}$ , as defined in Ref. 6, for  $\pi^+p$  and  $\pi^-p$  scattering at 6 GeV/c.<sup>27</sup> An experiment to measure the  $\pi^-p$  rotation parameters at 6 GeV/c is currently in the analysis stage<sup>28</sup> and further measurements are planned.

Finally, of course, extrapolations of our solution to 70 and 200 GeV/c, corresponding to the present Serpukhov and future Batavia accelerators, are full of interest. The predictions for  $\sigma_t$ ,  $\alpha$ ,  $d\sigma/dt$ , and  $P$  are contained in Figs. 24–26. These are fairly straightforward extrapolations, and their qualitative behavior holds no special surprises. The interest lies in the question, whether quantitative agreement with experiment will be found.

#### ACKNOWLEDGMENT

One of us (V. B.) thanks G. Weller for programming assistance.

<sup>27</sup> I. G. Aznauryan and L. D. Soloviev [Phys. Letters **28B**, 597 (1969)] have recently derived bounds on the rotation of polarization in  $\pi N$  scattering from dispersion sum rules.

<sup>28</sup> L. Van Rossum (private communication).